# Neutron-induced fission: properties of prompt neutron and $\gamma$ rays as a function of incident energy

I. Stetcu[1,a], P. Talou[1], and T. Kawano[1]

[1] *Theoretical Division, Los Alamos National Laboratory, Los Alamos, New Mexico, 87545, USA*

**Abstract.** We have applied the Hauser-Feshbach statistical theory, in a Monte-Carlo implementation, to the de-excitation of fission fragments, obtaining a reasonable description of the characteristics of neutrons and gamma rays emitted before beta decays toward stability. Originally implemented for the spontaneous fission of $^{252}$Cf and the neutron-induced fission of $^{235}$U and $^{239}$Pu at thermal neutron energy, in this contribution we discuss the extension of the formalism to incident neutron energies up to 20 MeV. For the emission of pre-fission neutrons, at incident energies beyond second-chance fission, we take into account both the pre-equilibrium and statistical pre-fission components. Phenomenological parameterizations of mass, charge and TKE yields are used to obtain the initial conditions for the fission fragments that subsequently decay via neutron and $\gamma$ emissions. We illustrate this approach for $^{239}$Pu(n,f).

## 1 Introduction

Applications often require the knowledge of prompt neutron and $\gamma$-ray spectra and other observables as a function of neutron incident energy for neutron-induced fission reactions. In this contribution, we describe the implementation of the incident neutron energy dependence into the CGMF (Cascading Gamma-ray and Multiplicity for Fission) code developed at Los Alamos for simulating prompt neutron and $\gamma$ observables.

In CGMF, the excited fission fragments are treated as compound nuclei, whose de-excitation is modeled in a Monte-Carlo implementation of the Hauser-Feshbach statistical decay model [1]. The Hauser-Feshbach framework provides the most detailed description of the de-excitation process. This approach requires knowledge of a large number of properties of far-from-stability nuclei, from density levels to neutron transmission coefficients or electromagnetic decay properties, in contrast to the Los Alamos model [2], which is based on a small number of parameters. However, in addition to the average neutron multiplicity and spectrum calculated in the Los Alamos model, CGMF provides many other observables, like neutron multiplicity distribution, $\gamma$-ray observables (average multiplicity and spectrum, multiplicity distribution), and spatial and energy correlation between prompt neutrons and/or $\gamma$ rays. Other codes that treat the de-excitation fission fragments via emission of neutrons and $\gamma$ rays are available [3–5].

In addition to the parameters that describe properties of the fission fragments, other quantities that directly relate to the fission itself are needed. CGMF does not simulate the dynamics of fission, and

[a] e-mail: stetcu@lanl.gov

thus the production of fission fragments. Hence, the mass, charge and total kinetic energy (TKE) distributions are taken from available experimental data or models. As data are scarce for other incident energies than thermal, we are forced to rely on systematics for neutron incident energies up to 20 MeV. The initial angular momentum distribution and the mechanism of the available total excitation energy (TXE) are quantities that are also necessary to perform Hauser-Feshbach simulations of the fission fragments. For these, experimental data provide only indirect evidence. Multi-chance fission probabilities (fission after the emission of one or more neutrons) are also required above about 5.5 MeV. We calculate the multi-chance fission probability by using the code CoH3 [6], and, depending on the fission barrier and nuclear structure parameters, the results can be closer or farther from the ENDF/B-VII.0 [7] evaluation. Only one set of multi-chance fission probabilities are considered here. The neutron emission is modeled by considering a mixture of pre-equilibrium (obtained using the exciton model [8–10]) and compound nucleus contributions. In this contribution, we concentrate in Sec. 2 on the evolution of mass, charge and TKE distribution parameters with the energy of the incident neutron, and leave the spin and sharing mechanism for a detailed discussion in future publications. The first results of the current implementation in CGMF for $^{239}$Pu(n,f) for incident energies up to 20 MeV are presented in Sec. 3, while a summary and outlook are presented in Sec. 4.

## 2 Energy dependence of mass and TKE distributions

The main assumptions in CGMF are that (i) the neutrons and $\gamma$ rays are only emitted from the fully accelerated fission fragments, (ii) no emission occurs during the evolution of the system between saddle and scission, or at the neck rupture, and (iii) the fission fragments are compound nuclei. Thus, in order to obtain the properties of neutrons and $\gamma$ rays, we start with a collection of fission fragments, which are sampled from a mass and charge distribution. Initially, CGMF has been developed only for the description of thermal neutron induced fission of $^{235}$U and $^{239}$Pu and the spontaneous fission of $^{252}$Cf [11, 12]. For these system the yield in mass and TKE, $Y(A, \mathrm{TKE})$, is directly available from experiment, or a host of data exist separately on mass yields, $Y(A)$, and average TKE and width as a function of primary fragment mass, so that $Y(A, \mathrm{TKE})$ can be constructed. In both cases, the charge distribution is taken from the Wahl systematics [13].

For the incident energy dependence of the fission fragments yields, we adopt the same five-Gaussian model as in Ref. [5], where the mass distribution is decomposed in fission modes whose parameters depend on the incident neutron energy $E_n$:

$$Y(A, E_n) = \frac{N_0}{\sqrt{2\pi}\sigma_0} e^{-\frac{(A-A_0)^2}{2\sigma_0^2}} + \sum_{i=1,2} \frac{N_i(E_n)}{\sqrt{2\pi}\sigma_i(E_n)} \left[ e^{-\frac{(A-A_0-D_i(E_n))^2}{2\sigma_i^2(E_n)}} + e^{-\frac{(A-A_0+D_i(E_n))^2}{2\sigma_i^2(E_n)}} \right]. \quad (1)$$

We take the same incident energy dependence for $D_i(E_n)$, $\sigma_i(E_n)$ and $N_i(E_n)$ as in Ref. [5]. For the symmetric mode, much less constrained than the asymmetric modes, the width of the distribution $\sigma_0$ does not vary with energy, and the only energy dependence comes from the normalization condition

$$N_0 + 2N_1(E_n) + 2N_2(E_n) = 2. \quad (2)$$

While we preserve the same energy dependence, we have modified the parameters of Ref. [5] at thermal energy for $^{235}$U(n,f) and $^{239}$Pu(n,f) to better agree with experimental data.

The fission yields parameterized in Eq. (1) are sampled and a list of possible fission fragments is generated. In the case of incident neutron energy above the threshold for multi-chance fission, we first simulate the emission of a number of neutrons according to the multi-chance fission probabilities. Both compound and preequilibrium emission components of the pre-fission neutron(s) are taken into

account. The emission has an important effect: not only it reduces the mass of the fissioning system, but also reduces the excitation energy available in the system. If the excitation energy in the fissioning system is below the fission barrier, we reject that event. A more detailed description will be presented in a future publication.

The TKE distribution is also needed in order to obtain the initial conditions for the fission fragments. A similar decomposition to Eq. (1) can be done for TKE, but the fit should include at the same time both the mass and TKE data. In this work, we assume that for each fragment fission $A$, the TKE distribution is a Gaussian characterized by the average $\langle \mathrm{TKE} \rangle(A, E_n)$ and width $\sigma_{\mathrm{TKE}}(A, E_n)$. This data is readily available for incident thermal neutron, and much more scarce for higher incident energies. However, in Fig. 1(a) we plot $\langle \mathrm{TKE} \rangle(A, E_n)$ scaled to $\langle \mathrm{TKE} \rangle(E_n)$ for a large number of fissioning systems and several neutron incident energies below the threshold for second-chance fission. This plot suggests that most of the energy dependence in $\langle \mathrm{TKE} \rangle(A, E_n)$ comes from the energy dependence of the average TKE, with little dependence on the particular isotope as well. Hence, we chose to relate the average TKE as a function of mass at an arbitrary incident neutron energy $E_n$ to be proportional to $\langle \mathrm{TKE} \rangle(A, E_{\mathrm{th}})$, i.e.,

$$\langle \mathrm{TKE} \rangle(A, E_n) = C(E_n)\, \langle \mathrm{TKE} \rangle(A, E_{\mathrm{th}}) \tag{3}$$

with the scaling constant determined so that the average TKE at that particular incident energy is reproduced:

$$\langle \mathrm{TKE} \rangle(E_n) = C(E_n) \sum_A Y(A, E_n) \times \langle \mathrm{TKE} \rangle(A, E_{\mathrm{th}}). \tag{4}$$

Here the summation runs only over the heavy fragment masses. Equation (3) is a first-order approximation, as a small, but systematic change in $\langle \mathrm{TKE} \rangle(A, E_n)$ is observed with increasing $E_n$. Taking into account that for large enough energies neutrons can be emitted before scission, $\langle \mathrm{TKE} \rangle(E_n)$ depends on the actual system that fission. We denote the mass of the fissioning system by $\mathcal{A} - n_{\mathrm{pre}}$, where $\mathcal{A}$ is the mass of the initial compound system (e.g., $\mathcal{A} = 240$ for the $^{239}$Pu(n,f) reaction) and $n_{\mathrm{pre}}$ is the number of neutrons emitted before fission. The Madland systematics [14] assumes the linear dependence of the average TKE with the neutron incident energy:

$$\langle \mathrm{TKE} \rangle(E_n) = E_0(\mathcal{A} - n_{\mathrm{pre}}) + s\, E_n, \tag{5}$$

where $s$ is a slope determined from experimental data below second-chance fission threshold, while $E_0$ is the average TKE at (equivalent) thermal neutron incident energy. The Madland parameterization is only valid below the second-chance fission, and, indeed, in the experimental data an increase in $\langle \mathrm{TKE} \rangle(E_n)$ is observed above the threshold for second-chance fission. However, we extend the same linear energy dependence of $\langle \mathrm{TKE} \rangle(E_n)$ up to 20 MeV, assuming that the slope $s$ is independent of the fissioning system, while $E_0(\mathcal{A})$ is determined so that we reproduce $\bar{\nu}$ at thermal energy for the $\mathcal{A}$ system. If neutrons are emitted prior to fission, we parameterize $E_0(\mathcal{A} - n_{\mathrm{pre}})$ as a function of the Coulomb parameter $\mathcal{Z}^2/(\mathcal{A} - n_{\mathrm{pre}})^{1/3}$, where $\mathcal{Z}$ is the charge of the compound fissioning system. For example, for $^{239}$Pu(n,f), we have obtained from fits to isotopes in the Pu chain

$$E_0(\mathcal{A} - n_{\mathrm{pre}}) = 178.6 - 0.4498 \left( \frac{94^2}{(\mathcal{A} - n_{\mathrm{pre}})^{1/3}} - 1423.8 \right). \tag{6}$$

Because the pre-scission neutrons carry energy, the energy of an equivalent incident neutron that would produce the fission of the $\mathcal{A} - n_{\mathrm{pre}}$ compound would be smaller. This explains the increase in TKE above the threshold for second-chance fission. Around those energies, the observed fissioning system is a superposition of the $\mathcal{A}$ and $\mathcal{A} - 1$ compounds, with the latter at a lower excitation energy.

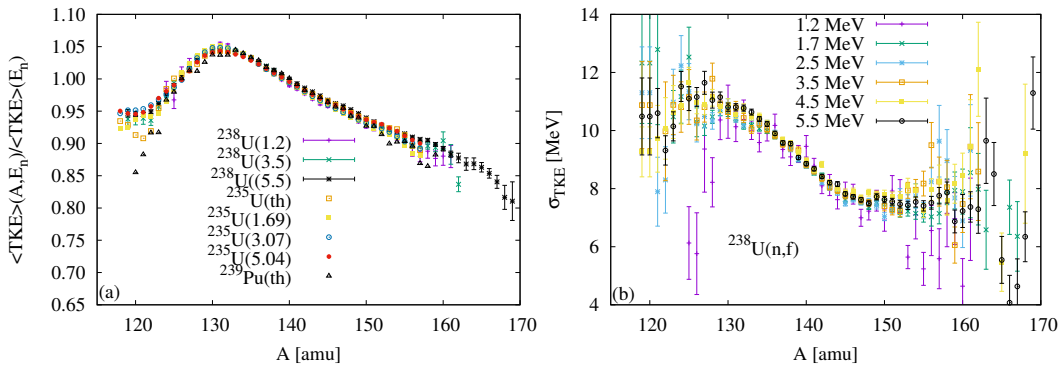


**Figure 1.** (a) The average TKE as a function of mass, scaled to the total average TKE for the neutron induced fission of $^{235}$U, $^{238}$U and $^{239}$Pu at several incident energies below the second-chance fission threshold. (b) The TKE width as a function of mass for several incident neutron energies in the case of the $^{238}$U(n,f) reaction.

The mixing is given by the fission probabilities and the result is an increase in TKE. With the simple extension of the linear behavior of $\langle \mathrm{TKE} \rangle$ with $E_n$ for each fissioning system, we can reproduce the features of the experimental data on $\langle \mathrm{TKE} \rangle(E_n)$ by only fitting $\bar{\nu}$ below the second-chance fission threshold. Thus, we can predict a large number of observables above the threshold to produce a neutron energy before fission without further adjustments. Finally, we assume no energy dependence of $\sigma_{\mathrm{TKE}}(A)$, as suggested by Fig. 1(b).

For a set of fission fragments generated by Eq. (1) we obtain the TKE by sampling the Gaussian distribution with the parameters $\langle \mathrm{TKE} \rangle(A)$ and $\sigma_{\mathrm{TKE}}(A)$ computed through the procedure outlined above. Once TKE is known, from the energetics of the reaction one can compute the total excitation energy (TXE) available to both fragments. The sharing of this energy is a complicated mechanism, and at this moment we utilize a parameterization that ensures a good reproduction of the average number of neutrons as a function of mass at thermal incident energy. Since more neutrons are emitted from the heavy fragments at higher incident energies, our model will not describe this feature correctly. However, this assumption does not change significantly the average of total neutrons emitted per fission event, $\bar{\nu}$. It also does not affect the $\gamma$-ray properties, since the residual energy available for $\gamma$ emission is controlled to a large extent by the average neutron separation energy. The implementation of a more sophisticated energy sharing mechanism is in progress.

$\bar{\nu}$ is extremely sensitive to TKE, as this quantity determines the energy available for neutron emissions. On the other hand, the competition between the neutron and $\gamma$-ray emissions also influences $\bar{\nu}$, but to a much smaller degree. In this implementation, we use the $\gamma$-neutron competition to fine tune $\bar{\nu}$ below the second-chance fission, via the parameter $\alpha$ that controls the initial spin distribution of the fission fragments (see Refs. [11, 12, 15] for a comprehensive discussion of the spin distributions). Thus, as in the case of TKE distribution parameters, we fit an energy dependence for $\alpha$ below the second-chance fission threshold only, which is then extended to 20 MeV incident neutron energy using multi-chance fission probabilities. More details regarding this parameterization will be given in a longer publication.

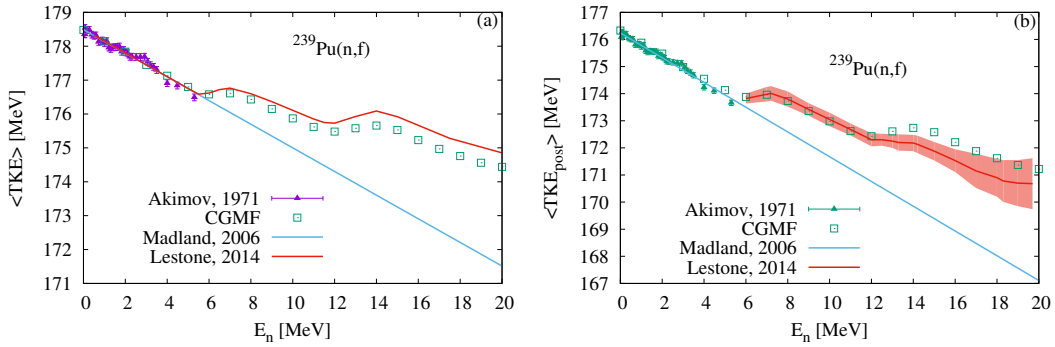


**Figure 2.** Pre-neutron emission (a) and post-neutron emission (b) average TKE of the fission fragments as a function of the neutron incident energy. We compare or results to the Madland systematics [14], valid up to 5.5 MeV, and the Lestone parameterization [16]. By construction, the Leston parameterization reproduces the Madland systematics below 5.5 MeV. For the post-neutron emission average TKE, we also show the uncertainty band for the Lestone parameterization.

## 3 Results for $^{239}$Pu(n,f)

In this section, we present our results in the case of $^{239}$Pu(n,f) reaction for $\langle \mathrm{TKE} \rangle(E_n)$, $\langle \mathrm{TKE}_{post} \rangle(E_n)$ (average fission fragment TKE after neutron emission), $\bar{\nu}(E_n)$, and $\langle E_\gamma^{tot} \rangle(E_n)$, where $\langle E_\gamma^{tot} \rangle$ is the total average $\gamma$-ray energy emitted per fission event. As discussed in Sec. 2, below the second-chance fission threshold, $\langle \mathrm{TKE} \rangle(E_n)$ is fitted to the Madland systematics [14], while $\bar{\nu}(E_n)$ to the ENDF values [7]. However, $\langle E_\gamma^{tot} \rangle(E_n)$ and $\langle \mathrm{TKE}_{post} \rangle(E_n)$ are predictions from 0 to 20 MeV, while $\langle \mathrm{TKE} \rangle(E_n)$ and $\bar{\nu}(E_n)$ are predictions above the threshold for the second-chance fission.

In Fig. 2, we present the predicted values for average TKE, pre- and post-neutron emissions. At thermal incident energy, the average pre-neutron emission TKE is shifted within recommended errors from the Madland value in order to obtain a good agreement with $\bar{\nu}$ (also fine tuned with $\alpha$). The emission of the pre-fission neutrons beyond the threshold for second-chance fission decreases the excitation energy in the fissioning system, and thus TKE, both pre- and post-neutron emission, increases. The final value of TKE depends on the multi-chance fission probabilities, which are not directly observable. We note, however, a reasonable agreement between the CGMF predictions and the Lestone parameterization [16] for both pre- and post-neutron emission TKE. Experimental data for the $^{239}$Pu(n,f) reaction for $\langle \mathrm{TKE}_{post} \rangle(E_n)$ exist from measurements with the SPIDER detector [17] at the Los Alamos Neutron Science Center and will be published shortly.

Figure 3(a) shows the dependence of $\bar{\nu}$ with the neutron incident energy. The good agreement between CGMF and ENDF suggests that our simple assumptions regarding the pre-neutron emission TKE are reasonable. We also obtain reasonable agreement between CGMF and available data for $\langle E_\gamma^{tot} \rangle$ up to 12 MeV, which is around the threshold for third-chance fission. Around this energy, CGMF starts to deviate with respect to the evaluated data. We note that the data below 5.5 MeV suggests an increase of the initial angular momentum with the neutron incident energy. At the second-chance fission threshold, the emission of a neutron decreases the excitation energy of the fissioning system and the initial angular momentum decreases (the probability to emit a neutron first and then fission increases quickly after the threshold). Hence, a small drop appears in the CGMF results for $\langle E_\gamma^{tot} \rangle$, and a plateau in the data, which remains consistent with the CGMF values. After the drop,

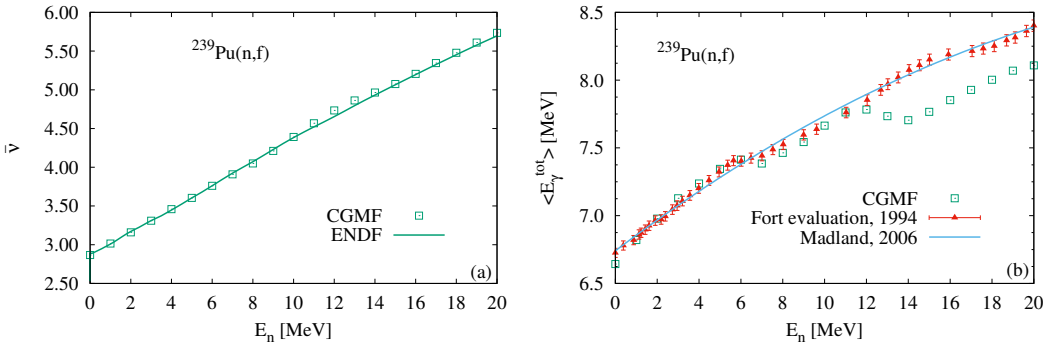


**Figure 3.** (a) CGMF and ENDF values of $\bar{\nu}$ as a function of incident neutron energy. (b) Comparison between CGMF and available data for $\langle E_\gamma^{tot} \rangle$ as a function of incident energy.

one expects that the angular momentum to increase, and a second drop to appear when the energetics will allow for a second neutron to be emitted before fission (third-chance fission threshold). This is where the CGMF results start to disagree with the data. This either suggest that our interpretation of the behavior of the initial spin distribution with increasing the incident neutron energy is incorrect and something happens around third-chance fission threshold, or the data, which have not been published in a peer-reviewed journal, are suspicious. Future measurements of this quantity would be thus quite useful in order to guide the models.

## 4 Summary and outlook

For neutron-induced fission reactions we have extended the range of applicability of CGMF from thermal energies up to 20 MeV incident neutron energy. The mass yields and charge are taken from systematics, while above the threshold for second-chance fission, we simulate the emission of one or more neutrons before the fission process occurs, considering the competition between pre-equilibrium and compound nucleus emission. The fragments are considered compound nuclei, whose de-excitation is described within the Hauser-Feshbach formalism. We have assumed that the same $\langle \mathrm{TKE} \rangle(A)$, measured at thermal incident energy, can be used over the full range of incident energies, scaled to reproduce the TKE systematics of Madland, extended to 20 MeV for each fissioning system. The widths $\sigma_{\mathrm{TKE}}(A)$ of the distribution have been taken the same over for all the incident energies. After we fit the average neutron multiplicity below 5.5 MeV to the ENDF values, we predicted several observables up to 20 MeV. Thus, we obtain a good reproduction of $\bar{\nu}$ up to 20 MeV, and of the total average $\gamma$-ray energy up to 12 MeV. Average TKE, pre- and post-neutron emission is also consistent with available data and current models.

Other available theoretical models for the mass [18, 19] and TKE [20] yields can be incorporated into our approach. Moreover, we work currently on the implementation of a more accurate mechanism for the sharing of the excitation energy between the fission fragments. This will allow us to more realistically predict the mass-dependent average neutrons emitted per fission event. In parallel with these developments, we will study the sensitivity of our results with respect to the input parameters as some observables will be more sensitive to some parameters than others. Finally, the current implementation can be extended to more isotopes as well as photo-fission reactions.

## Acknowledgements

We thank R. Vogt and J. Randrup for useful discussions and for providing us with the parameters for the mass yields. This work was performed at Los Alamos National Laboratory, under the auspices of the National Nuclear Security Administration of the U.S. Department of Energy at Los Alamos National Laboratory under contract No. DE-AC52-06NA25396. We acknowledge partial support from the Office of Defense Nuclear Nonproliferation Research & Development (DNN R&D), National Nuclear Security Administration, US Department of Energy.

## References

[1] W. Hauser, H. Feshbach, Phys. Rev. **87**, 366 (1952)
[2] D.G. Madland, J.R. Nix, Nucl. Sci. Eng. **81**, 213 (1982)
[3] K.H. Schmidt, B. Jurado, Tech. rep. (2015), `http://www.khs-erzhausen.de/GEF.html`
[4] D. Regnier, Ph.D. thesis, Université de Grenoble (2013)
[5] R. Vogt, J. Randrup, D.A. Brown, M.A. Descalle, W.E. Ormand, Phys. Rev. C **85**, 024608 (2012)
[6] T. Kawano, P. Talou, M.B. Chadwick, T. Watanabe, J. Nucl. Sci. Tech. **47**, 462 (2010)
[7] M. Chadwick, P. Obložinský, M. Herman, N. Greene, R. McKnight, D. Smith, P. Young, R. MacFarlane, G. Hale, S. Frankle et al., Nuclear Data Sheets **107**, 2931 (2006), evaluated Nuclear Data File ENDF/B-VII.0
[8] C. Kalbach, Phys. Rev. C **33**, 818 (1986)
[9] C. Kalbach, Phys. Rev. C **71**, 034606 (2005)
[10] A. Koning, M. Duijvestijn, Nuclear Physics A **744**, 15 (2004)
[11] B. Becker, P. Talou, T. Kawano, Y. Danon, I. Stetcu, Phys. Rev. C **87**, 014617 (2013)
[12] I. Stetcu, P. Talou, T. Kawano, M. Jandel, Phys. Rev. C **90**, 024617 (2014)
[13] A.C. Wahl, Report LA-13928, Los Alamos National Laboratory (2002)
[14] D. Madland, Nuclear Physics A **772**, 113 (2006)
[15] I. Stetcu, P. Talou, T. Kawano, M. Jandel, Phys. Rev. C **88**, 044603 (2013)
[16] J. Lestone, T. Strother, Nuclear Data Sheets **118**, 208 (2014)
[17] F. Tovesson, C.W. Arnold, T. Bredeweg, M. Jandel, A.B. Laptev, K. Meierbachtol, A. Sierk, W. M., A.A. Hecht, D. Mader et al., *SPIDER: A new instrument for fission yield measurement*, in *Proceedings of the Fifth International Conference on ICFN5*, edited by J.H. Hamilton, A.V. Ramayya (World Scientific, 2013), p. 361
[18] J. Randrup, P. Möller, Phys. Rev. Lett. **106**, 132503 (2011)
[19] J. Randrup, P. Möller, A.J. Sierk, Phys. Rev. C **84**, 034613 (2011)
[20] A. Sierk, Report LA-UR-14-27056, Los Alamos National Laboratory (2014)